Journal of Electrical Engineering & Technology Vol. 7, No. 4, pp. 513~523, 2012 **513**
http://dx.doi.org/10.5370/JEET.2012.7.4.513

LMI-based Sliding Mode Speed Tracking Control Design for Surface-mounted Permanent Magnet Synchronous Motors

Viet Quoc Leu*, Han Ho Choi* and Jin-Woo Jung†

Abstract – For precisely regulating the speed of a permanent magnet synchronous motor system with unknown load torque disturbance and disturbance inputs, an LMI-based sliding mode control scheme is proposed in this paper. After a brief review of the PMSM mathematical model, the sliding mode control law is designed in terms of linear matrix inequalities (LMIs). By adding an extended observer which estimates the unknown load torque, the proposed speed tracking controller can guarantee a good control performance. The stability of the proposed control system is proven through the reachability condition and an approximate method to implement the chattering reduction is also presented. The proposed control algorithm is implemented by using a digital signal processor (DSP) TMS320F28335. The simulation and experimental results verify that the proposed methodology achieves a more robust performance and a faster dynamic response than the conventional linear PI control method in the presence of PMSM parameter uncertainties and unknown external noises.

Keywords: Permanent magnet synchronous motor (PMSM), Sliding mode control, Robust control, Speed control, Load torque observer, Linear matrix inequality (LMI)

1. Introduction

Among various types of ac motors, the permanent magnet synchronous motor (PMSM) has received widespread acceptance in industry owing to high dynamic performance and high efficiency [1-3]. Conventionally, the linear control schemes such as PI controller and LQ regulator have been widely used in industrial motor drives because of their relatively simple implementation [2-4]. However, the PMSM systems have nonlinear characteristics and always encounter various disturbances in actual applications (e.g., unmodeled dynamics, parameter uncertainties, and unknown external disturbances). Accordingly, the linear control methods cannot accomplish a high performance such as fast transient response, no overshoot, zero steady-state error, and robustness in case that there exist PMSM parameter uncertainties and unknown external disturbances.

On the other hand, the nonlinear control strategies can become an alternative solution to accurately track the reference trajectory of the PMSM. Recently, some nonlinear control algorithms such as robust control [5], fuzzy control [6], adaptive control [7, 8], sliding mode control [9, 10], have been presented. In [5], the H_∞ robust control strategy has been designed based on the reduced-order dynamic model of the PMSMs, but the model does not include the load torque term and its robustness has not been fully verified. Also, the fuzzy speed controller has been proposed, which the load torque is considered [6]. However, its design method requires too many fuzzy rules to approximate the nonlinear system, making the analysis excessively complex. Some adaptive controllers have been reported [7, 8], and the control performance shows acceptable results. Nevertheless, the controller design procedures are still quite complicated. Particularly, sliding mode control (SMC) has emerged as one of the most effective methods which can achieve good speed control performance for the PMSMs because it is insensitive to system uncertainties and disturbances. Unfortunately, traditional SMC often leads to the chattering control input due to its discontinuous switching control. To cope with this challenge, SMC with boundary layer [9] or SMC with a continuously varying term [10] has been presented. However, the chattering phenomenon of the switching control signal may still appear under certain operating conditions.

Since the 1990s, linear matrix inequalities (LMIs) have been extensively applied to control problems because of the following great advantages [11]:

(1) Many engineering optimization problems can be easily formulated as LMI problems;
(2) If a control problem is converted to an LMI, then any local solution is a global optimum;
(3) Various numerical LMI solvers can be used to economically solve optimization problems;
(4) Once a control problem is transformed to an LMI, any other useful LMI performance constraints can be easily added to the problem.

From the above advantages of SMC and LMIs, this

† Corresponding Author: Division of Electronics and Electrical Engineering, Dongguk University-Seoul, Korea. (jinwjung@dongguk.edu)
* Division of Electronics and Electrical Engineering, Dongguk University-Seoul, Korea.
Received: April 15, 2011; Accepted: April 29, 2012

paper presents an LMI-based sliding mode speed controller for the PMSM drives. The proposed control methodology compensates for the disturbance inputs which are neglected in most previous PMSM drives [9, 10]. The stability of the closed-loop control system is analyzed and an approximation method is also discussed for chattering reduction. Furthermore, a simple load torque observer is employed to exactly estimate the unknown load toque disturbance. The overall control algorithm is implemented on a prototype PMSM driving system with a TI TMS320F28335 DSP. It is verified through simulations and experiments that the proposed LMI-based sliding mode controller guarantees a more robust performance and a faster dynamic response than the conventional linear PI controller in the presence of motor parameter uncertainties and external disturbances.

This paper is organized as follows. In Section 2, the mathematical model of PMSM is described. In Section 3, the LMI-based sliding mode speed controller is designed and the stability is analytically proven. The load torque observer is addressed in Section 4. Then, the observer-based sliding mode speed controller is derived in Section 5. To verify the effectiveness of the proposed method, the simulation and experimental results are presented in Section 6. Finally, conclusion is given in Section 7.

2. Mathematical Model of PMSM

By taking the rotor flux axis as the *d*-axis in the synchronously rotating *dq* reference frame, a surface-mounted PMSM is characterized by the following nonlinear model.

$$\begin{aligned}\dot{\omega} &= k_1 i_{qs} - k_2\omega - k_3 T_L \\ \dot{i}_{qs} &= -k_4 i_{qs} - k_5\omega + k_6 V_{qs} - i_{ds}\omega + d_1(t) \\ \dot{i}_{ds} &= -k_4 i_{ds} + k_6 V_{ds} + i_{qs}\omega + d_2(t)\end{aligned} \tag{1}$$

where

V_{ds}, V_{qs}	: *d*-axis and *q*-axis stator voltages (V);
i_{ds}, i_{qs}	: *d*-axis and *q*-axis stator currents (A);
ω	: electrical rotor angular velocity (rad/sec);
θ	: rotor position (rad);
R_s	: stator resistance (Ω);
L_s	: stator inductance (H);
J	: rotor equivalent inertia (kg·m^2);
B	: viscous friction coefficient (N·m·sec/rad);
λ_m	: magnetic flux (V·sec/rad);
p	: number of poles;
T_L	: load torque (N·m);
$d_1(t)$, $d_2(t)$	: disturbance inputs representing the system uncertainties and external disturbances.

and the parameters $k_i > 0$ (i = 1, …, 6) are determined by R_s, L_s, J, B, λ_m, p. That is, each k_i is defined as follows:

$$k_1 = \frac{3}{2J}\frac{p^2}{4}\lambda_m,\ k_2 = \frac{B}{J},\ k_3 = \frac{p}{2J}$$
$$k_4 = \frac{R_s}{L_s},\ k_5 = \frac{\lambda_m}{L_s},\ k_6 = \frac{1}{L_s}$$

In this paper, we suppose the following things to design an LMI-based sliding mode speed controller as the previous methods:

A1) ω, i_{ds}, and i_{qs} are measurable.

A2) T_L is unknown. For a fixed sampling interval, the external load does not change abruptly. Thus, its derivative $\dot{T}_L$ can be disregarded [12].

A3) The speed reference ω_d is constant, so $\dot{\omega}_d = \ddot{\omega}_d = 0$.

3. LMI-based Sliding Mode Speed Controller Design and Stability Analysis

3.1 Control system model description

Introduce desired *q*-axis current i_{qsd} as

$$i_{qsd} = \left(k_2\omega_d + \dot{\omega}_d + k_3 T_L\right)/k_1 \tag{2}$$

The position error, speed error and *q*-axis current error can be calculated as the following equations:

$$\tilde{\theta} = \int_0^t (\omega - \omega_d)\,d\tau,\ \tilde{\omega} = \omega - \omega_d,\ \tilde{i}_{qs} = i_{qs} - i_{qsd} \tag{3}$$

Using (1) to (3), the system Eq. (1) is rewritten as

$$\begin{aligned}\dot{\tilde{\theta}} &= \tilde{\omega} \\ \dot{\tilde{\omega}} &= k_1\tilde{i}_{qs} - k_2\tilde{\omega} \\ \dot{\tilde{i}}_{qs} &= -k_4 i_{qs} - k_5\omega + k_6 V_{qs} - i_{ds}\omega - \dot{i}_{qsd} + d_1(t) \\ \dot{i}_{ds} &= -k_4 i_{ds} + k_6 V_{ds} + i_{qs}\omega + d_2(t)\end{aligned} \tag{4}$$

Let the control inputs V_{qs} and V_{ds} be decomposed as

$$\begin{aligned}V_{qs} &= \left(u_{1f} + u_1\right) \\ V_{ds} &= \left(u_{2f} + u_2\right)\end{aligned} \tag{5}$$

where u_{1f}, u_{2f} are the nonlinear decoupling control law to compensate for the nonlinear dynamics of PMSM, and u_1, u_2 are the switching control law to force the system trajectory to the sliding surface.

The linearizing control law u_{1f}, u_{2f} are defined as

$$\begin{aligned}u_{1f} &= \left(k_4 i_{qs} + k_5\omega + i_{ds}\omega + \dot{i}_{qsd}\right)/k_6 \\ u_{2f} &= -i_{qs}\omega/k_6\end{aligned} \tag{6}$$

So the model (2) can be simplified as follows:

$$\begin{aligned}\dot{\tilde{\theta}} &= \tilde{\omega} \\ \dot{\tilde{\omega}} &= k_1 \tilde{i}_{qs} - k_2 \tilde{\omega} \\ \dot{\tilde{i}}_{qs} &= k_6 u_1 + d_1(t) \\ \dot{i}_{ds} &= -k_4 i_{ds} + k_6 u_2 + d_2(t)\end{aligned} \tag{7}$$

The dynamic model (7) can be expressed as the following state-space equation

$$\dot{x} = Ax + B[u + u_d] \tag{8}$$

where

$$A = \begin{bmatrix} 0 & 1 & 0 & 0 \\ 0 & -k_2 & k_1 & 0 \\ 0 & 0 & 0 & 0 \\ 0 & 0 & 0 & -k_4 \end{bmatrix}, \quad B = \begin{bmatrix} 0 & 0 \\ 0 & 0 \\ k_6 & 0 \\ 0 & k_6 \end{bmatrix}, \quad x = \begin{bmatrix} \tilde{\theta} \\ \tilde{\omega} \\ \tilde{i}_{qs} \\ i_{ds} \end{bmatrix}^T,$$

$$u = [u_1 \quad u_2]^T, \; u_d = \frac{1}{k_6}[d_1(t) \quad d_2(t)]^T.$$

3.2 Sliding surface and switching law design

Let Φ be defined as an orthonormal basis for the null space of B^T, i.e., a 4×2 full column rank matrix such that

$$\Phi^T B = 0, \; \Phi^T \Phi = I \tag{9}$$

Also, Φ can be easily computed by using Matlab command "null" as follows

$$\Phi = null(B') \tag{10}$$

In the closed-loop control system (8), $A \in R^{4\times4}$ and $B \in R^{4\times2}$ are constant matrices. Assuming that the following LMI condition is feasible

$$X > 0, \; \Phi^T (AX + XA^T) \Phi < 0 \tag{11}$$

Then the sliding surface is given by

$$\sigma = Sx = (B^T X^{-1} B)^{-1} B^T X^{-1} x = 0 \tag{12}$$

where S is a 2×4 matrix and $X \in R^{4\times4}$ is a solution matrix to the LMI condition (11).

Here, an assumption is added as follows:

A4) $d_1(t)$, $d_2(t)$ are unknown, but bounded as

$$\|u_d\| \le \rho_u \|u\| + \rho_f(t) \tag{13}$$

where $0 \le \rho_u < 1$ is a known constant, and $\rho_f(t)$ is a known nonnegative function.

Then the switching control law is designed as

$$u = -S \cdot Ax - k \cdot \mathrm{sgn}(\sigma) \tag{14}$$

where $k > (\varepsilon + \rho_f + \rho_u \|S \cdot Ax\|)/(1 - \rho_u)$ and $\varepsilon > 0$.

3.3 Stability analysis

Generally, stability analysis of a sliding mode control system is divided into two steps. That is, the stability of the reduced-order sliding mode dynamics is shown. Then the reachability condition is verified.

Firstly, the transformation matrix M and the associated vector z are defined as the following:

$$\begin{aligned} M &\triangleq \begin{bmatrix} (\Phi^T X \Phi)^{-1} \Phi^T \\ (B^T X^{-1} B)^{-1} B^T X^{-1} \end{bmatrix} = \begin{bmatrix} V \\ S \end{bmatrix}, \\ z &\triangleq \begin{bmatrix} z_1 \\ z_2 \end{bmatrix} = \begin{bmatrix} Vx \\ Sx \end{bmatrix} = Mx \end{aligned} \tag{15}$$

where $z_1 \in R^2$, $z_2 \in R^2$. It is easy to see that $M^{-1} = [X \; \Phi \; B]$ and $z_2 = \sigma$, then $z = [z_1 \; \sigma]^T$.

Thus, the time derivative of z is calculated as

$$\begin{aligned} \dot{z} &= M\dot{x} = MAx + MB(u + u_d) \\ &= MAM^{-1} z + MB(u + u_d) \end{aligned} \tag{16}$$

Then the closed-loop control system (8) can be transformed into the following regular form

$$\begin{bmatrix} \dot{z}_1 \\ \dot{\sigma} \end{bmatrix} = \begin{bmatrix} VAX\Phi & VAB \\ SAX\Phi & SAB \end{bmatrix} \begin{bmatrix} z_1 \\ \sigma \end{bmatrix} + \begin{bmatrix} 0 \\ I \end{bmatrix} [u + u_d] \tag{17}$$

On the other hand, from the equivalent control method of Utkin [13], we can see that the equivalent control law is given by

$$u_{eq}(t) = -SAx - u_d(t) \tag{18}$$

By setting $\dot{\sigma} = \sigma = 0$ and substituting $u(t)$ with $u_{eq}(t)$, we can show that the reduced second-order sliding mode dynamics restricted to the switching surface (12) is expressed as

$$\dot{z}_1 = (\Phi^T X \Phi)^{-1} \Phi^T AX\Phi z_1 \tag{19}$$

The sliding mode dynamics (19) is asymptotically stable

if there exists a positive definite matrix $P_1 \in R^{2\times2}$ such that the time derivative of the Lyapunov function $V(z_1, t) = z_1^T P_1 z_1$ satisfies for some positive scalar κ

$$\dot{V} = z_1^T \left[A_1^T P_1 + P_1 A_1 \right] z_1 \le -\kappa \|z_1\|^2 \tag{20}$$

where $A_1 = (\Phi^T X \Phi)^{-1} \Phi^T A X \Phi$. This implies that (19) is asymptotically stable if there exists a positive definite matrix $P_1 \in R^{2\times2}$ such as

$$A_1^T P_1 + P_1 A_1 < 0 \tag{21}$$

Let the positive definite matrix P_1 be $P_1 = \Phi^T X \Phi$, where X is a solution matrix to the LMI (11), then the matrix inequality (21) is equivalent to the LMI (11). Therefore, the Lyapunov inequality (20) holds with $P_1 = \Phi^T X \Phi > 0$, which implies that the reduced-order sliding mode dynamics (19) is asymptotically stable.

Secondly, the reachability condition $\sigma^T \cdot \dot{\sigma}$ is satisfied for all $\sigma \neq 0$ as follows:

$$\begin{aligned}
\sigma^T \cdot \dot{\sigma} &= \sigma^T (S \cdot A x + u + u_d) \\
&= \sigma^T (-k \cdot \mathrm{sgn}(\sigma) + u_d) \\
&= -k\|\sigma\| + \sigma^T u_d \\
&\le -k\|\sigma\| + \|\sigma\|(\rho_u \|u\| + \rho_f) \\
&\le -k\|\sigma\| + \|\sigma\|\left[\rho_u (\|S \cdot Ax\| + k) + \rho_f\right] \\
&= -\left((1-\rho_u)k - \rho_u \|S \cdot Ax\| - \rho_f\right)\|\sigma\| \\
&< -\varepsilon \|\sigma\|
\end{aligned} \tag{22}$$

Also, the following equality is used.

$$\begin{aligned}
\dot{\sigma} &= -S\dot{x} = \left(B^T P_1 B\right)^{-1} B^T P_1 \dot{x} \\
&= \left(B^T P_1 B\right)^{-1} B^T P_1 \left(Ax + B(u + u_d)\right) \\
&= S \cdot A x + (u + u_d)
\end{aligned} \tag{23}$$

Therefore, the reachability condition (22) proves the following theorem.

Theorem 1: Consider the closed-loop system of (1). Then, the sliding mode control law (5) with (6) and (14) guarantees the asymptotic stability of $x = 0$ in spite of the disturbance inputs $d_1(t)$ and $d_2(t)$.

3.4 Chattering reduction

In fact, chattering still exists when the sliding mode control law (5) with (6) and (14) is applied. To suppress the chattering phenomenon in the real applications, the discontinuous function can be replaced by a continuous approximation such as $\sigma/(\|\sigma\| + \delta)$ where $\delta > 0$. As δ converges to zero, the approximated control law is arbitrarily close to that of the original control law.

Thus, the switching control law (14) can be approximated to the following equation:

$$u = -S \cdot A x - k \frac{\sigma}{(\|\sigma\| + \delta)} \tag{24}$$

where $\delta > 0$.

Finally, the control inputs V_{qs} and V_{ds} can be expressed with (6) and (24) as

$$\begin{aligned}
V_{qs} &= \frac{1}{k_6}\left(k_4 i_{qs} + k_5 \omega + i_{ds}\omega + \dot{i}_{qsd}\right) - G_1 x - k \frac{\sigma_1}{(\|\sigma\| + \delta)} \\
V_{ds} &= -\frac{1}{k_6} i_{qs}\omega - G_2 x - k \frac{\sigma_2}{(\|\sigma\| + \delta)}
\end{aligned} \tag{25}$$

where $S \cdot A = G = [G_1\ G_2]^T$.

Based on (5), (6), (24), (25), Fig. 1 shows a schematic diagram of the proposed LMI-based sliding mode controller.

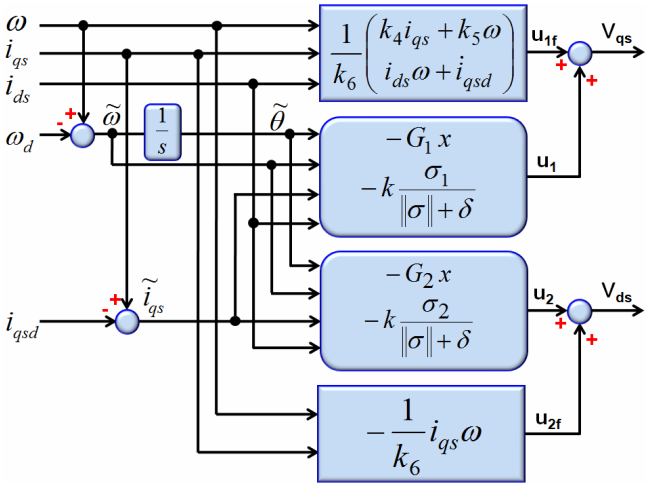

Fig. 1. Schematic diagram of the proposed LMI-based sliding mode controller.

4. Load Torque Observer Design

As expected previously, the proposed sliding mode control law (25) includes the load torque T_L term. It means that the control performance can be severely affected by the load torque variations if T_L is not properly observed. In this section, a simple load torque observer is utilized to know its information.

From (1) and *A2*, the following second-order equation is obtained

$$\begin{aligned} \dot{T}_L &= 0 \\ \dot{\omega} &= -k_2\omega + k_1 i_{qs} - k_3 T_L \end{aligned} \tag{26}$$

This can be rewritten as the state-space form below

$$\dot{x}_o = A_o x_o + B_o u_o \tag{27}$$

where $x_o = \begin{bmatrix} T_L \\ \omega \end{bmatrix}$, $A_o = \begin{bmatrix} 0 & 0 \\ -k_3 & -k_2 \end{bmatrix}$, $B_o = \begin{bmatrix} 0 \\ 1 \end{bmatrix}$, and $u_o = k_1 i_{qs}$.

Then the load torque observer can be represented as the following state-space model

$$\begin{aligned} \dot{\hat{x}}_o &= A_o \hat{x}_o + L y_o - L C_o \hat{x}_o + B_o u_o \\ y_o &= C_o x_o \\ \hat{T}_L &= C_T \hat{x}_o \end{aligned} \tag{28}$$

where $\hat{T}_L$ is an estimate of T_L, and $L \in R^{2\times 1}$ is an observer gain matrix, and

$$\hat{x}_o = \begin{bmatrix} \hat{T}_L & \hat{\omega} \end{bmatrix}^T, \quad C_o = \begin{bmatrix} 0 & 1 \end{bmatrix}, \quad C_T = \begin{bmatrix} 1 & 0 \end{bmatrix}$$

The error dynamics of the load torque observer can be obtained as follows

$$\dot{\tilde{x}}_o = \left[A_o - L C_o\right]\tilde{x}_o \tag{29}$$

where $\tilde{x}_o = x_o - \hat{x}_o$.

Theorem 2: Assume that the following LMI condition is feasible

$$P_o > 0, \;\; P_o A_o - Y_o C_o + A_o^T P_o - C_o^T Y_o^T < 0 \tag{30}$$

where $P_o \in R^{2\times 2}$ and $Y_o \in R^{2\times 1}$ are decision variables.

Also, assume that the load torque observer gain matrix L is calculated by

$$L = P_o^{-1} Y_o \tag{31}$$

Then, the estimation error converges exponentially to zero.

Proof: Assume that the LMI (30) is feasible. Then there exists a matrix $Q_o > 0$ such that

$$P_o A_o - Y_o C_o + A_o^T P_o - C_o^T Y_o^T < -Q_o < 0 \tag{32}$$

Let us define the Lyapunov function as $V_o(\tilde{x}_o) = \tilde{x}_o^T P_o \tilde{x}_o$. Its time derivative using the error dynamics (29) is given by

$$\begin{aligned} \dot{V}_o(\tilde{x}_o) &= \frac{d}{dt}\left[\tilde{x}_o^T P_o \tilde{x}_o\right] = 2\tilde{x}_o^T \left[P_o A_o - P_o L C_o\right]\tilde{x}_o \\ &= 2\tilde{x}_o^T \left[P_o A_o - P_o P_o^{-1} Y_o C_o\right]\tilde{x}_o = 2\tilde{x}_o^T \left[P_o A_o - Y_o C_o\right]\tilde{x}_o \\ &= \tilde{x}_o^T \left[P_o A_o - Y_o C_o + A_o^T P_o - C_o^T Y_o^T\right]\tilde{x}_o \\ &\le -\tilde{x}_o^T Q_o \tilde{x}_o \end{aligned} \tag{33}$$

Then this implies that $\tilde{x}_o$ is exponentially stable.

5. Observer-based Sliding Mode Speed Controller

If an estimated load torque $\hat{T}_L$ is used instead of T_L, the q-axis current error is estimated as follows:

$$\hat{\tilde{i}}_{qs} = i_{qs} - \hat{i}_{qsd} = i_{qs} - \left(k_2\omega_d + \dot{\omega}_d + k_3\hat{T}_L\right)/k_1 \tag{34}$$

The observer-based control law V_{qs} and V_{ds}, which includes a sliding mode speed regulator and a load torque observer, can be rewritten as

$$\begin{aligned} V_{qs} &= \frac{1}{k_6}\left(k_4 i_{qs} + k_5\omega + i_{ds}\omega + \dot{i}_{qsd}\right) - G_1\hat{x} - k\frac{\sigma_1}{\left(\|\sigma\| + \delta\right)} \\ V_{ds} &= -\frac{1}{k_6} i_{qs}\omega - G_2\hat{x} - k\frac{\sigma_2}{\left(\|\sigma\| + \delta\right)} \end{aligned} \tag{35}$$

where $\hat{x} = \left[\tilde{\theta}, \tilde{\omega}, \hat{\tilde{i}}_{qs}, i_{ds}\right]^T$.

Remark 1: Because the sliding surface parameter matrix S and the load torque observer gain matrix L are characterized by using LMIs, various useful convex performance criteria such as quadratic performance, H_2/H_∞ performance bounds can be handled in designing S and L. For example, if the LMI (30) is replaced with

$$\gamma I > P_o > 0, \;\; P_o A_o - Y_o C_o + A_o^T P_o - C_o^T Y_o^T + Q_o < 0 \tag{36}$$

where $Q_o \ge 0$, then a load torque observer gain L guaranteeing the LQ performance bound constraint $\int_0^\infty \tilde{x}_o^T Q_o \tilde{x}_o \, dt \le \gamma$ for any $\| \tilde{x}_o \| \le 1$ can be designed.

Here, the proposed sliding mode speed controller will be implemented in the simulation and experiment.

6. Performance Evaluations

6.1 Control system gains

In order to validate the effectiveness of the proposed control system, simulations and experiments have been

carried out. The nominal parameters of a prototype PMSM used in this paper are given: rated power P_{rated} = 1 HP; rated phase current I_{rated} = 3.94 A; rated torque T_{rated} = 3.9 N·m; p = 12; R_s = 0.99 Ω; L_s = 5.82 mH; $\lambda_m = 7.92\times10^{-2}$ V·sec/rad; $J = 12.08\times10^{-4}$ kg·m^2; $B = 3\times10^{-4}$ N·m·sec/rad.

Assume that the disturbance inputs $d_1(t) = 0.6\cdot k_6\cdot\sin(2\pi\cdot50\cdot t) = 103.09\cdot\sin(2\pi\cdot50\cdot t)$ and $d_2(t) = -0.6\cdot k_6\cdot\sin(2\pi\cdot50\cdot t) = -103.09\cdot\sin(2\pi\cdot50\cdot t)$, it means the bounded disturbance $\|u_d\|\le 0.6$. Thus, the dynamic model (1) can be expressed as

$$\begin{aligned}\dot{\omega} &= 3539.60\, i_{qs} - 0.25\,\omega - 4968.80\, T_L \\ \dot{i}_{qs} &= -170.10\, i_{qs} - 13.60\,\omega + 171.82\, V_{qs} - i_{ds}\omega \\ &\quad + 103.09\,\sin(2\pi\cdot 50\cdot t) \\ \dot{i}_{ds} &= -170.10\, i_{ds} + 171.82\, V_{ds} + i_{qs}\omega \\ &\quad + 103.09\,\sin(2\pi\cdot 50\cdot t)\end{aligned} \tag{37}$$

The q-axis current error can be estimated as

$$\hat{\tilde{i}}_{qs} = i_{qs} - \left(0.25\,\omega_d + \dot{\omega}_d + 4968.8\,\hat{T}_L\right)/3539.6 \tag{38}$$

By solving the LMI condition (30), the solution (P_o, Y_o) can be obtained as the following

$$P_o = \begin{bmatrix} 0.0040 & 0.0031 \\ 0.0031 & 0.0029 \end{bmatrix}, \quad Y_o = \begin{bmatrix} -16.7794 \\ 8.4763 \end{bmatrix} \tag{39}$$

From (31), the load torque observer gain matrix L is derived as

$$L = \begin{bmatrix} -31622.8 \\ 36252.4 \end{bmatrix} \tag{40}$$

Referring to (6), the nonlinear decoupling control law u_{1f} and u_{2f} can be given by

$$\begin{aligned} u_{1f} &= 0.9900\, i_{qs} + 0.0792\,\omega + 0.0058\, i_{ds}\,\omega \\ u_{2f} &= -0.0058\, i_{qs}\,\omega \end{aligned} \tag{41}$$

Finally, the observer-based sliding mode control law u_1 and u_2 is represented as the following

$$\begin{aligned} u_1 &= -G_1\hat{x} - k\frac{\sigma_1}{(\|\sigma\| + \delta)} \\ u_2 &= -G_2\hat{x} - k\frac{\sigma_2}{(\|\sigma\| + \delta)} \end{aligned} \tag{42}$$

It is noted that the parameters k and δ are designed on the basis of the common control engineering knowledge [14]. If k is too big, the chattering may not be completely eliminated, while if k is too small, the steady-state error may happen. Also, the steady-state error may occur when δ is too large. However, if δ is too small, the chattering still remains. Therefore, the parameters uncertainties should be chosen suitably according to each particular control system. In (42), k = 250, δ = 0.1, and the matrix G is designed as

$$G = \begin{bmatrix} G_1 \\ G_2 \end{bmatrix} = \begin{bmatrix} 0 & -0.0001 & 1.5170 & 0 \\ 0 & 0 & 0 & -0.9900 \end{bmatrix} \tag{43}$$

6.2 Simulation results

To evaluate the proposed control algorithm, simulations have been made using Matlab/Simulink under two conditions below:

Case 1) The desired speed (ω_d) decreases from 157.08 rad/sec to –157.08 rad/sec at 0.3 sec and then increases from –157.08 rad/sec to 157.08 rad/sec at 0.7 sec. In this case, the motor parameters are nominal, and T_L is 2 N·m;

Case 2) The desired speed (ω_d) decreases from 157.08 rad/sec to –157.08 rad/sec at 0.3 sec and then increases from –157.08 rad/sec to 157.08 rad/sec at 0.7 sec. In this case, some parameters (R_s, L_s, B, and J) and load torque T_L are changed to half the nominal values, i.e., R_s = 0.495 Ω, L_s = 2.91 mH, $B = 1.5\times10^{-4}$ N·m·sec/rad, $J = 6.04\times10^{-4}$ N·m·sec/rad, T_L = 1 N·m.

Figs. 2 and 3 show the simulation results of the proposed sliding mode controller under Case 1 and Case 2, respectively. Each figure shows the desired speed (ω_d), the measured speed (ω), the d-axis current (i_{ds}), the q-axis current (i_{qs}), the phase a current (i_a), the load torque (T_L), and the estimated load torque ($\hat{T}_L$). In both figures, the speed transient response has no overshoot and a short settling time (0.008 sec), and the steady-state speed error is almost zero.

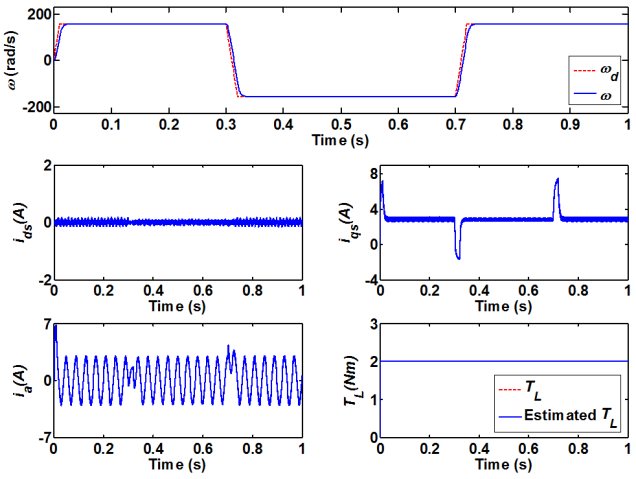

Fig. 2. Simulation results with the proposed controller under nominal parameters.

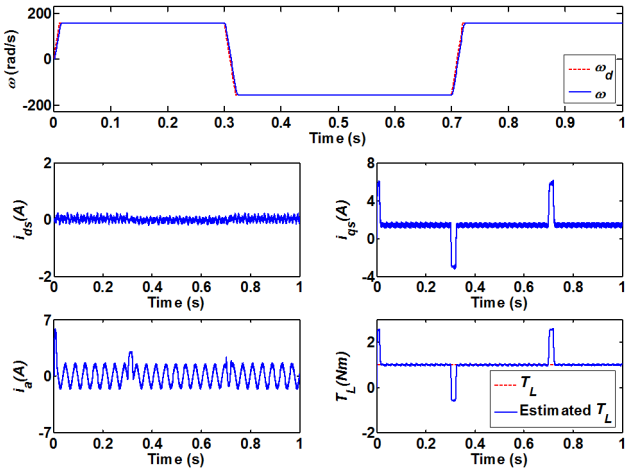

Fig. 3. Simulation results with the proposed controller when some parameters (R_s, L_s, B, and J) and load torque T_L are changed to half the nominal values.

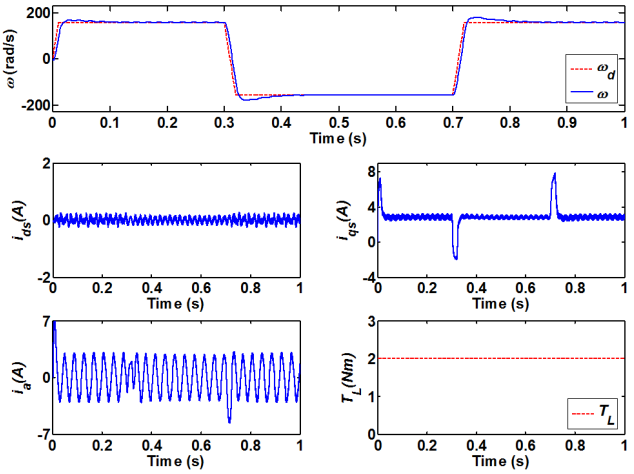

Fig. 4. Simulation results with the PI-PI controller under nominal parameters.

For comparisons, the conventional control method with a PI speed controller in an outer loop and a PI current controller an inner loop has been simulated under the same conditions as the proposed control method. As shown in Table 1, the PI gains of the current controller and the speed controller are determined by the tuning rules [15, 16]. It is noted that the gains are closely related to the system parameters. In this paper, the bandwidth of each PI controller is designed as ω_I = 2π·150 rad/sec and ω_ω = 2π·15 rad/sec, respectively. Figs. 4 and 5 show the simulation results of the conventional PI-PI controller under Case 1 and Case 2, respectively. In the figures, we can find bigger overshoot and longer settling time in the transient response compared to the proposed method: 14.15 % and 0.07 sec under nominal parameters and 27.19 % and 0.102 sec under some parameter variations.

Table 1. PI gains for current controller and speed controller

Each PI controller		$K_p + K_i/s$
Current Loop (Subscript "I")	P Gain (K_{pI})	$K_{pI} = L_s\omega_I = 5.49$
	I Gain (K_{iI})	$K_{iI} = R_s\omega_I = 933.05$
Speed Loop (Subscript "ω")	P Gain ($K_{p\omega}$)	$K_{p\omega} = 2\omega_\omega/k_I = 0.05$
	I Gain ($K_{i\omega}$)	$K_{i\omega} = \omega_\omega^2/k_I/2 = 1.25$

From Figs. 2 to 5, the proposed controller gives a better transient performance such as no overshoot and fast settling time in comparison to the conventional PI-PI controller. Note that the disturbance inputs do not influence the proposed control scheme; meanwhile, they still occur in the PI-PI control scheme.

6.3 Experimental results

In this section, the experimental results are presented to verify the feasibility of the proposed sliding mode control scheme. Fig. 6 illustrates the block diagram of overall

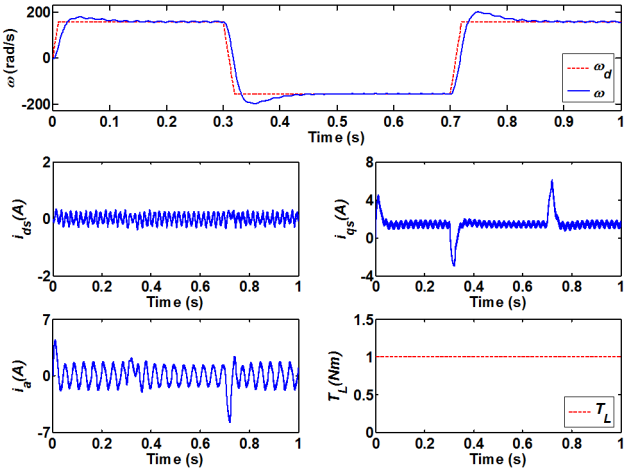

Fig. 5. Simulation results with the PI-PI controller when some parameters (R_s, L_s, B, and J) and load torque T_L are changed to half the nominal values.

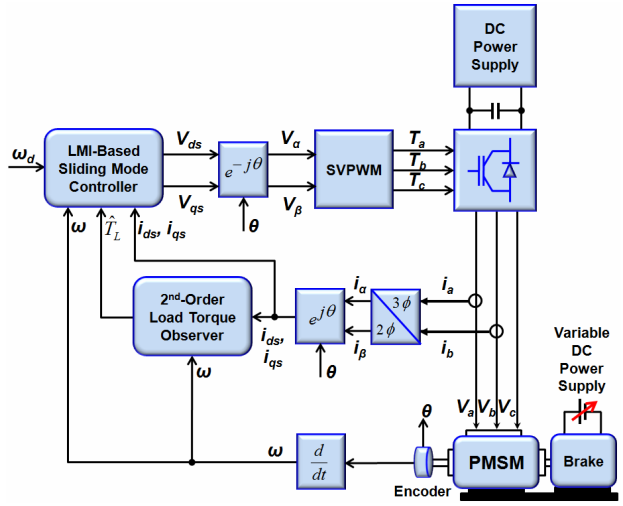

Fig. 6. Block diagram of overall PMSM driving system.

PMSM driving system which consists of a three-phase inverter with TI DSP TMS320F28335, a surface-mounted PMSM, and a brake for load torque. For a three-phase IGBT inverter, a FSBS5CH60 600V/5A smart power module manufactured by Fairchild Semiconductor is used as the power switches. It is noted that an LMI-based sliding mode speed controller and a load torque observer have been fully implemented on the TMS320F28335.

As shown in Fig. 6, the proposed sliding mode controller has only a speed control loop that includes the dynamics of d-axis and q-axis currents. Two phase currents (i_a, i_b) and the rotor position (θ) are measured via current sensors and an encoder, respectively. Considering the system efficiency and control performance, the sampling frequency and the switching frequency are selected as 5 kHz. Also, a space vector PWM (SVPWM) is utilized among various PWM methods. Fig. 7 shows the configuration of experimental testbed.

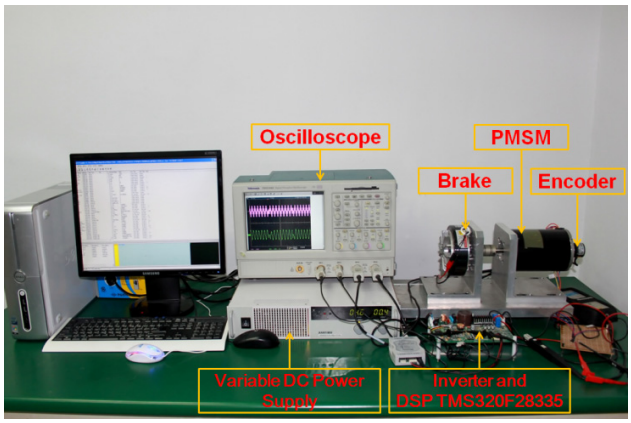

Fig. 7. Configuration of experimental testbed.

Figs. 8 and 9 show the experimental results of the proposed LMI-based sliding mode controller and conventional PI-PI controller under the same conditions (Case 1) as Figs. 2 and 4, respectively. Figs. 10 and 11 show the experimental results of the proposed LMI-based sliding mode controller and conventional PI-PI controller under the same conditions (Case 2) as Figs. 3 and 5, respectively. Figs. 8(a) through 11(a) illustrate the measured speed (ω), desired speed (ω_d), and speed error ($\tilde{\omega}$). Figs. 8(b) through 11(b) show the d-axis current (i_{ds}) and q-axis current (i_{qs}). Figs. 8(c) through 11(c) show the load torque (T_L), estimate ($\hat{T}_L$) of the load torque, and phase a current (i_a).

Thus, the experimental results definitely demonstrate that the proposed control strategy ensures the faster transient response and better robust performance than the conventional PI-PI control method.

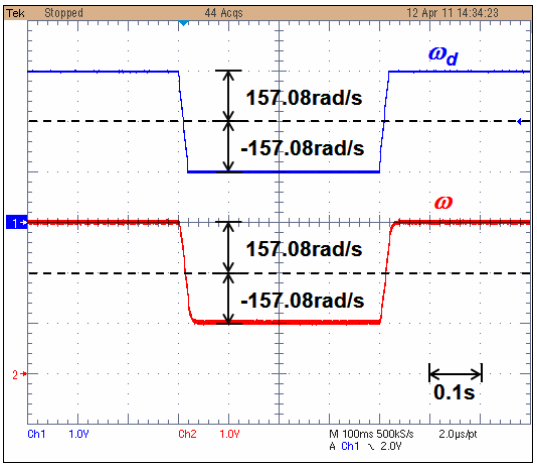

(a) Desired speed (ω_d) and measured speed (ω)

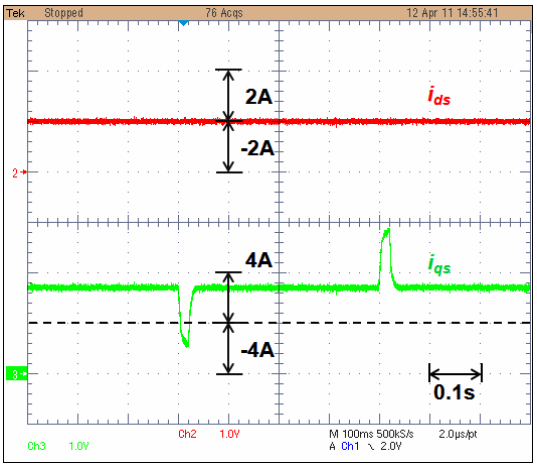

(b) d-axis current (i_{ds}) and q-axis current (i_{qs})

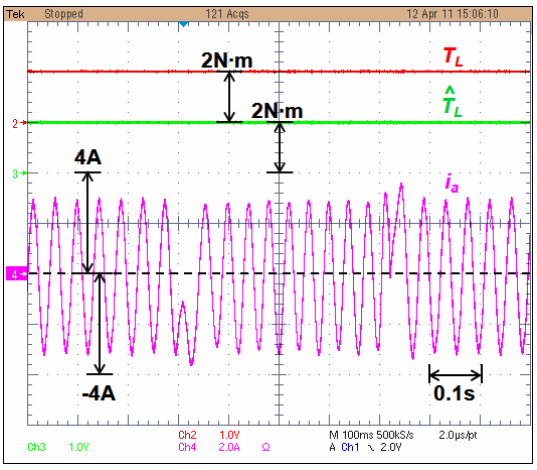

(c) Phase a current (i_a), load torque (T_L), and estimated load torque ($\hat{T}_L$)

Fig. 8. Experimental results with the proposed LMI-based sliding mode controller under nominal parameters.

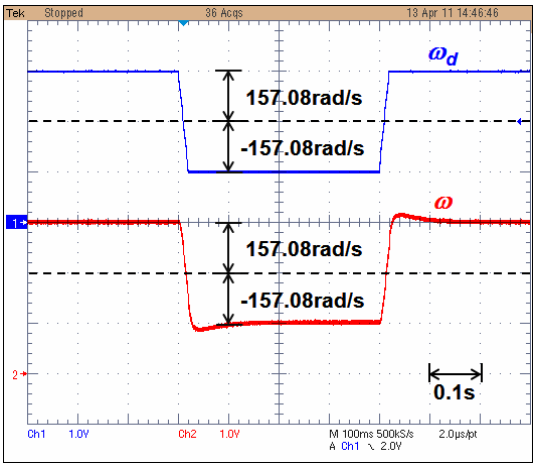

(a) Desired speed (ω_d) and measured speed (ω)

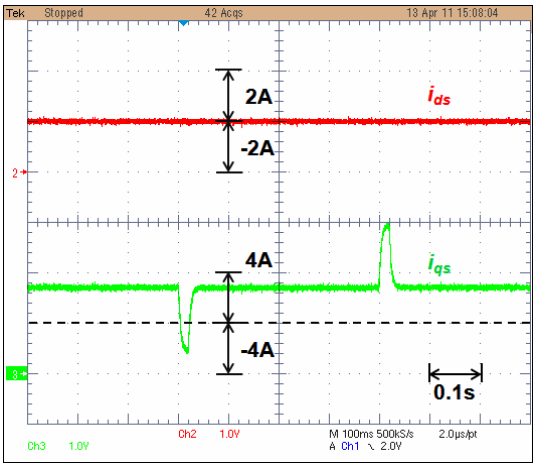

(b) d-axis current (i_{ds}) and q-axis current (i_{qs})

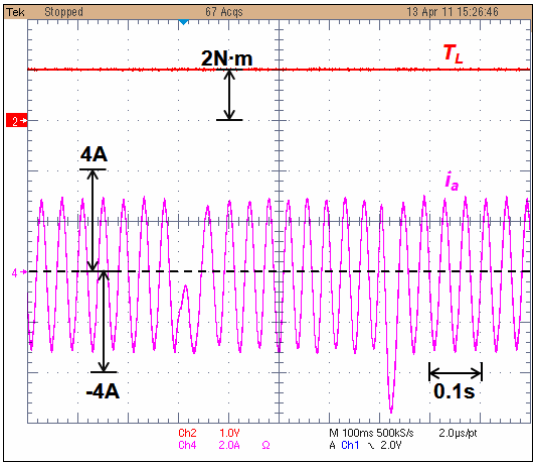

(c) Phase a current (i_a), load torque (T_L), and estimated load torque ($\hat{T}_L$)

Fig. 9. Experimental results with the conventional PI-PI control under nominal parameters.

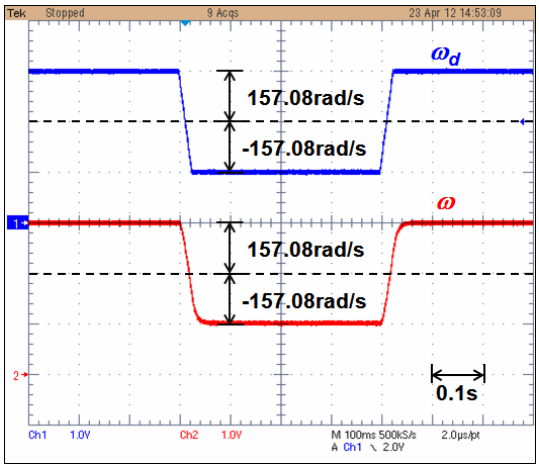

(a) Desired speed (ω_d) and measured speed (ω)

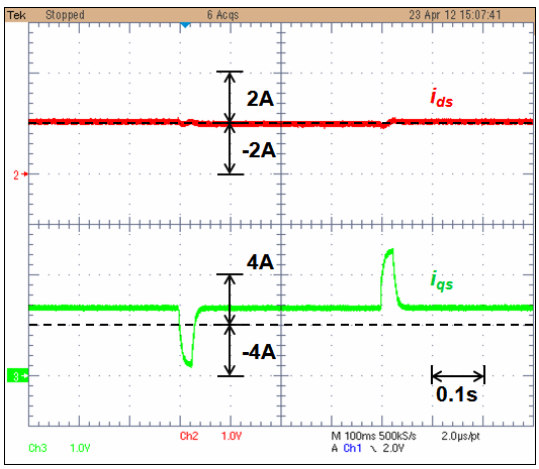

(b) d-axis current (i_{ds}) and q-axis current (i_{qs})

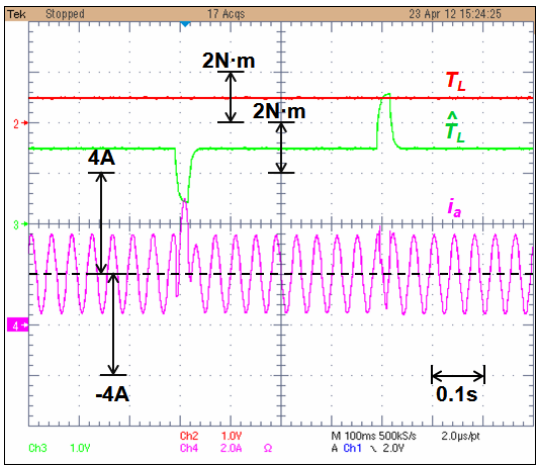

(c) Phase a current (i_a), load torque (T_L), and estimated load torque ($\hat{T}_L$)

Fig. 10. Experimental results with the proposed LMI-based sliding mode controller when some parameters (R_s, L_s, B, and J) and load torque T_L are changed to half the nominal values.

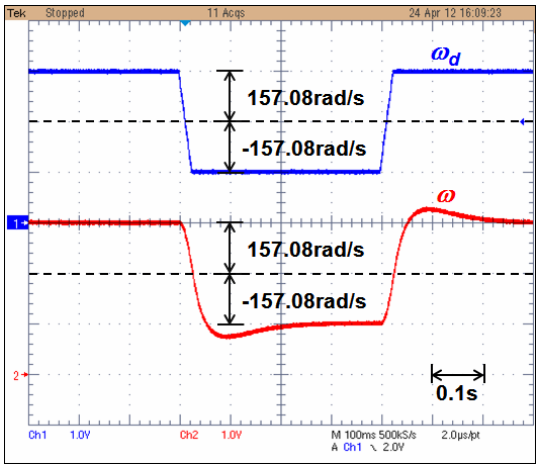

(a) Desired speed (ω_d) and measured speed (ω)

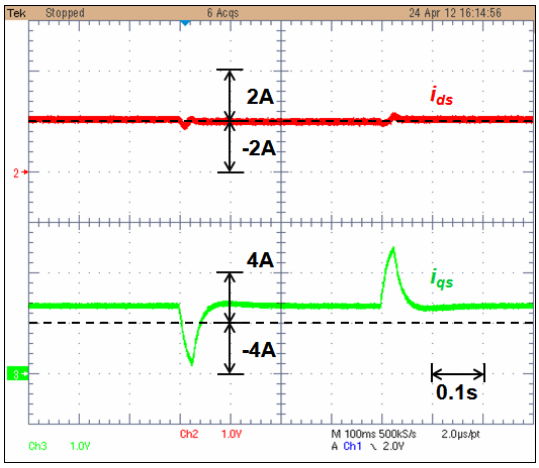

(b) d-axis current (i_{ds}) and q-axis current (i_{qs})

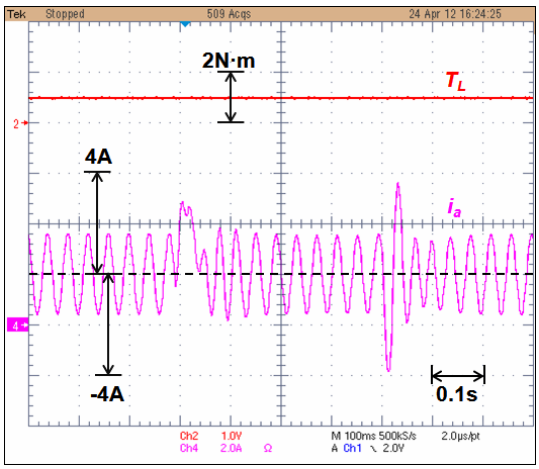

(c) Phase a current (i_a), load torque (T_L), and estimated load torque ($\hat{T}_L$)

Fig. 11. Experimental results with the conventional PI-PI controller when some parameters (R_s, L_s, B, and J) and load torque T_L are changed to half the nominal values.

7. Conclusion

This paper proposes an LMI-based sliding mode controller for speed tracking of a PMSM. The proposed controller considers the external disturbances that are neglected in most previous PMSM drives. The stability of the proposed control system is analytically verified. The approximated control law is implemented to suppress the chattering effect which occurs in the original sliding control law. The whole control algorithm has been fully realized using TMS320F28335. The simulation and experimental results have proved that the proposed control methodology can achieve not only the fast transient response but also the better robust control performance in comparison with the conventional PI-PI control scheme in the presence of PMSM parameter uncertainties and unknown external noises.

Acknowledgements

This work was supported by the Energy Efficiency & Resources of the Korea Institute of Energy Technology Evaluation and Planning (KETEP) grant funded by the Ministry of Knowledge Economy, Republic of Korea (No. 2010T100200468).

References

[1] G. Zhou and J. W. Ahn, "A novel efficiency optimization strategy of IPMSM for pump applications," *Journal of Electrical Engineering & Technology*, Vol. 4, No. 4, pp. 515-520, Dec. 2009.

[2] H. S. Kang, C. K. Kim, and Y. S. Kim, "Position control for interior permanent magnet synchronous motors using an adaptive integral binary observer," *Journal of Electrical Engineering & Technology*, Vol. 4, No. 2, pp. 240-248, Jun. 2009.

[3] J. G. Lee, K. H. Nam, S. H. Lee, S. H. Choi, and S. W. Kwon, "A lookup table based loss minimizing control for FCEV permanent magnet synchronous motors," *Journal of Electrical Engineering & Technology*, Vol. 4, No. 2, pp. 201-210, Jun. 2009.

[4] Y. Yan, J. G. Zhu, and Y. G. Guo, "Initial rotor position estimation and sensorless direct torque control of surface-mounted permanent magnet synchronous motors considering saturation saliency," *IET Electr. Power Appl.*, Vol. 2, No. 1, pp. 42-48, Jan. 2008.

[5] T. L. Hsien, Y. Y. Sun, and M. C. Tsai, "H_∞ control for a sensorless permanent-magnet synchronous drive," *Proc. Inst. Elect. Eng.-Electr. Power Appl.*, Vol. 144, No. 3, pp. 173-181, May 1997.

[6] K. Y. Lian, C. H. Chiang, and H. W. Tu, "LMI-based sensorless control of permanent-magnet synchronous motors," *IEEE Trans. Ind. Electron.*, Vol. 54, No. 5,

pp. 2769-2778, Oct. 2007.
[7] F. J. Lin and P. H. Chou, "Adaptive control of two-axis motion control system using interval type-2 fuzzy neural network," *IEEE Trans. Ind. Electron.*, Vol. 56, No. 1, pp. 178-193, Jan. 2009.
[8] Y. A. R. I. Mohamed, "Adaptive self-tuning speed control for permanent-magnet synchronous motor drive with dead time," *IEEE Trans. Energy Conversion*, Vol. 21, No. 4, pp. 855-862, Dec. 2006.
[9] I. C. Baik, K. H. Kim, and M. J. Youn, "Robust nonlinear speed control of PM synchronous motor using boundary layer integral sliding mode control technique," *IEEE Tran. Cont. Syst. Tech*., Vol. 8, No. 1, pp. 47-54, Jan. 2000.
[10] D. Q. Zhang and S. K. Panda, "Chattering-free and fast-response sliding mode controller," *IEE Proc.-Control Theory Appl.,* Vol. 146, No. 2, pp.171-177, Mar. 1999.
[11] J. F. Camino, J. W. Helton, and R. E. Skelton, "Solving matrix inequalities whose unknowns are matrices," *IEEE CDC*, Vol. 3, pp. 3160-3166, Dec. 2004.
[12] C. K. Lin, T. H. Liu, and S. H. Yang, "Nonlinear position controller design with input-output linearisation technique for an interior permanent magnet synchronous motor control system," *IET Power Electron.*, Vol. 1, No. 1, pp. 14-26, Mar. 2008.
[13] V. I. Utkin, "Variable structure systems with sliding modes", *IEEE Trans. Autom. Control*, Vol. 22, No. 2, pp. 212-222, Apr 1977.
[14] J. W Jung, Y. S. Choi, V. Q. Leu, and H. H. Choi, "Fuzzy PI-type current controllers for permanent magnet synchronous motors," *IET Electr. Power Appl*., Vol. 5, No. 1, pp. 143-152, Jan. 2011.
[15] H. Z. Jin and J. M. Lee, "An RMRAC current regulator for permanent magnet synchronous motor based on statistical model interpretation," *IEEE Trans. Ind. Electron*., Vol. 56, No. 1, pp. 169-177, Jan. 2009.
[16] P. Kshirsagar, R. P. Burgos, A. Lidozzit, J. Jang, F. Wang, D. Boroyevich, and S. K. Sul, "Implementation and sensorless vector-control design and tuning strategy for SMPM machines in fan-type applications," *IEEE Industry Appl. Conf.*, Vol. 4, pp. 2062-2069, Oct. 2006.

Viet Quoc Leu received the B.S. and M.S. degrees in electrical engineering from Hanoi University of Technology, Hanoi, Vietnam in 2006 and 2008, respectively. He is currently pursuing the Ph.D. degree in the Division of Electronics and Electrical Engineering, Dongguk University, Seoul, Korea. His research interests are in the field of DSP-based electric machine drives and control of distributed generation systems using renewable energy sources.

Han Ho Choi received the B.S. degree in control and instrumentation engineering from Seoul National University, Seoul, Korea, in 1988, and the M.S. and Ph.D. degrees in electrical engineering from Korea Advanced Institute of Science and Technology, Daejeon, Korea, in 1990 and 1994, respectively. From 1994 to 1998, he was a Team Leader with the Advanced Technology Laboratory, DaeWoo Electrical Company. He is currently with the Division of Electronics and Electrical Engineering, Dongguk University, Seoul, Korea. His research interests include linear-matrix-inequality-based control system design, microprocessor-based control systems, variable structure systems, and microprocessor-based electric machine drives.

Jin-Woo Jung received the B.S. and M.S. degrees in Electrical Engineering from Hanyang University, Seoul, Korea in 1991 and 1997, respectively, and the Ph.D. degree in Electrical and Computer Engineering from The Ohio State University, Columbus, Ohio, USA, in 2005. From 1997 to 2000, he was with the Digital Appliance Research Laboratory, LG Electronics Co., Ltd., Seoul, Korea. From 2005 to 2008, he worked at the R&D Center and PDP Development Team, Samsung SDI Co., Ltd., Korea, as a senior engineer. Since 2008, he has been an Associate Professor with the Division of Electronics and Electrical Engineering, Dongguk University, Seoul, Korea. His current research interests are in the area of DSP-based electric machine drives, control of distributed generation systems using renewable energy sources (wind turbines, fuel cells, solar cells), design and control of power converters, driving circuits and driving methods of ac plasma display panels (PDP).